Very High-Resistance Fault on a 525 kV Transmission Line – Case Study

Paulo Koiti Maezono
Virtus Consultoria e Serviços Ltda.

Enrique Altman and Kennio Brito
Transener Internacional Ltda.

Vanessa Alves dos Santos Mello Maria
ATE Transmissora de Energia Ltda.

Fabiano Magrin
Schweitzer Engineering Laboratories, Inc.

Very High-Resistance Fault on a 525 kV Transmission Line – Case Study

Paulo Koiti Maezono, *Virtus Consultoria e Serviços Ltda.*
Enrique Altman and Kennio Brito, *Transener Internacional Ltda.*
Vanessa Alves dos Santos Mello Maria, *ATE Transmissora de Energia Ltda.*
Fabiano Magrin, *Schweitzer Engineering Laboratories, Inc.*

Abstract—This paper analyzes a 300 ohm primary ground fault, which is an unusually high value for a 525 kV transmission line in southeastern Brazil. This case study emphasizes the techniques used by the analysts.

Considering that the fault impedance was larger than those usually observed in single-phase faults on extra-high-voltage (EHV) lines, this paper discusses the probable cause of the fault and mentions an analysis technique to evaluate such faults. The protective relaying community lacks information regarding the causes and values of fault resistances to ground on high-voltage (HV) and EHV transmission lines. The objectives of this paper are to stimulate research and contribute to the collection of very high-resistance fault information.

The analysis techniques are presented using symmetrical components and fault calculations to arrive at fault parameter values that are very close to the ones provided by protective relays. The performance of the line protection is evaluated for the specific fault conditions, with calculation of the observed impedances and currents. The importance of the ground over-current directional protection on a pilot directional comparison scheme is shown. Speculation on the widespread use of differential protection for transmission lines should stimulate discussions of line protection philosophies and applications.

The criteria for the resistive reach setting of the quadrilateral ground distance characteristic are presented to show an evolution of past criteria and to open discussion about the setting limits.

The conclusions of this paper highlight the importance of present event report analysis techniques regarding fault calculation software and the need for appropriate settings criteria for the resistive ground distance element threshold. This paper also supports the use of ground directional overcurrent protection with a pilot scheme for HV and EHV transmission line protection, while proposing the widespread use of differential functions for transmission lines, even for the most extensive cases.

I. INTRODUCTION

This paper is based on the event report analysis of five faults on a 525 kV single-circuit transmission line located in southeastern Brazil. The 121.4-kilometer transmission line interconnects the SE Assis Terminal to the SE Londrina Terminal in São Paulo and Paraná States, as shown in Fig. 1. Transener Internacional Ltda. is responsible for operating this transmission line.
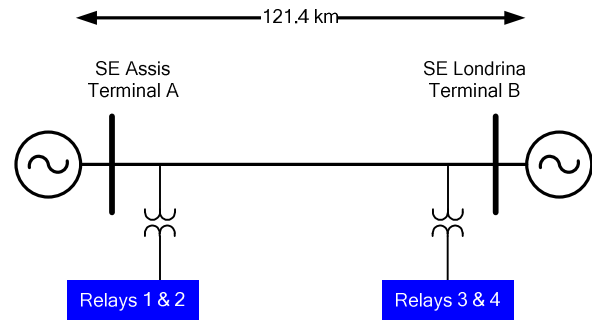
Fig. 1.   525 kV transmission line from SE Assis Terminal A to SE Londrina Terminal B, located in southeastern Brazil

Transener uses a dual main protection system at each terminal. The characteristics of the relays are mho for phase elements and mho and quadrilateral for ground elements. The backup protection uses a DCUB (directional comparison unblocking) scheme with mho Zone 2 phase and ground characteristics and a ground directional overcurrent for high-resistance faults.

The first three faults happened on the same day in July 2006 and two others in August 2006. The line between the cities of Assis and Londrina crosses the Paranapanema River. The line has a positive-sequence impedance of $Z1 = 2.50 + j\,38.65$ ohms primary and a zero-sequence impedance of $Z0 = 44.27 + j\,170.32$ ohms primary.

This paper describes the analysis techniques and the computational tool used to analyze the first fault. For the other faults, the numeric and comparative results are presented, using the same methodology as the first analysis. The nature of the fault, the estimated value of the fault resistance (R_F), and the estimated fault location on the transmission line are presented for each fault. The apparent impedances at each extremity of the transmission line are calculated using event report data.

The performance of the transmission line protection is evaluated for the observed conditions. From that evaluation, we see the importance of the pilot directional ground overcurrent protection for high-voltage (HV) and extra-high-voltage (EHV) lines. The widespread use of the differential function as the main protection for a transmission line could effectively replace conventional schemes and theories.

II. ANALYSIS OF JULY 2006 FAULTS

On the same day in July 2006, three faults occurred: the first one at 12:36 p.m., the second at 12:47 p.m., and the third at 12:58 p.m. At the time, the cause of these faults was unknown.

All three faults were high-impedance B-phase-to-ground faults, and all three faults were cleared by ground directional overcurrent elements of the pilot scheme.

A. Analysis of First Fault

1) Nature of the Fault

The first fault was characterized as a high-impedance fault with gradually rising ground current. Several cycles after the start of the fault, the current reached the minimum protection threshold. Fig. 2 displays the ground fault current as seen from Terminal A.
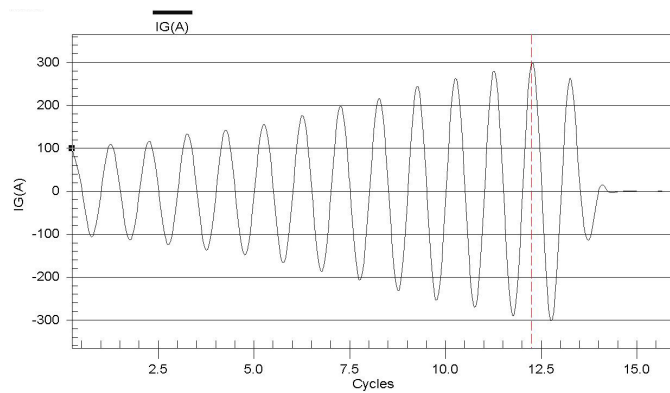
Fig. 2. Ground current at Terminal A

Fig. 3 displays the voltage and current phasors as seen from Terminal A at the moment the relay tripped. There was practically no voltage sag for the faulted phase. With a high-impedance fault (hundreds of ohms), the angular difference between the B-phase voltage and the B-phase current is between −5° and −10°. Fig. 3 shows a predominantly resistive characteristic.
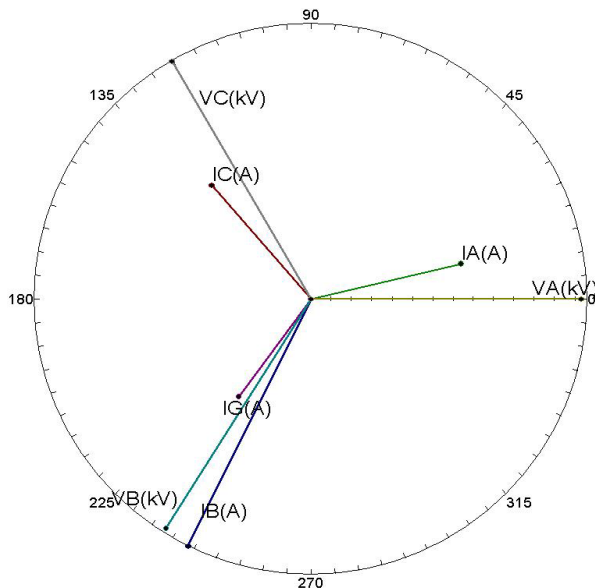
Fig. 3. Voltage and current phasors

When the observed current presents such a resistive angle, the fault is a high-impedance (resistance) type. The I_B phasor is the sum of the prefault load current and the Thèvenin's short-circuit current.

I_{Ground} (Terminal A) = 299.5 A ∠ −4.5° (related to VB)

I_{Ground} (Terminal B) = 266.9 A ∠ −3.3° (related to VB)

2) Fault Current and Thèvenin's Current at Terminal A

The event report shows the total fault current measured by the protective relay. Using the superposition principle, the total current is the result of the prefault load current added to Thèvenin's current.

For the event under analysis, the prefault currents (positive sequence) and voltages are listed in Table I.

TABLE I
TERMINAL A PREFAULT VOLTAGES AND CURRENTS

	Magnitude	Angle	Real	Imaginary
I_{1A} (A)	379.8	236.2	−211.28	−315.61
I_{1B} (A)	379.8	116.2	−167.68	340.78
I_{1C} (A)	379.8	−3.8	378.96	−25.17
V_{1A} (kV)	312.4	225.6	−218.57	−223.20
V_{1B} (kV)	312.4	105.6	−84.01	300.89
V_{1C} (kV)	312.4	−14.4	302.59	−77.69

Table II lists the B-phase fault current and voltage at Terminal A.

TABLE II
TERMINAL A VOLTAGE AND CURRENT AT RELAY TRIP INSTANT

	Magnitude	Angle	Real	Imaginary
I_B (A)	680.8	112.2	−257.23	630.33
V_B (kV)	309.8	110	−105.96	291.12
I_N (A)	299.5	100.10	−52.52	294.86

For the Thèvenin's current calculation, the positive-sequence current of the faulted phase is adjusted to be equal to the measured negative-sequence current, as shown in Table III.

TABLE III
NEGATIVE SEQUENCES USING THÈVENIN'S CURRENT

	Magnitude (A)	Angle	Comments
I_{2A}	109.50	−20.5	
I_{2B}	109.50	99.5	From Event Report
I_{2C}	109.50	219.5	
I_{1A}	109.50	219.5	
I_{1B}	109.50	99.5	Adopted Equal to I2B
I_{1C}	109.50	−20.5	
I_{0A}	99.83	100.1	
I_{0B}	99.83	100.1	From Event Report
I_{0C}	99.83	100.1	

Thèvenin's current is $I_{Bth} = I_{1B} + I_{2B} + I_{0B}$. The fault current is equal to Thèvenin's current added to the prefault current, as shown in Table IV.

TABLE IV
TERMINAL A TOTAL FAULT CURRENT

	Magnitude (A)	Angle
I_F Thev (IB)	318.83	99.69
+		
I Prefault	379.80	116.20
=		
I_F Total	691.44	108.67
From Event Report	680.80	112.20

The calculated current differs by just 1.54 percent from the measured current.

3) Fault Current and Thèvenin's Current at Terminal B
The prefault currents at Terminal B are listed in Table V.

TABLE V
TERMINAL B PREFAULT VOLTAGE AND CURRENTS

	Magnitude	Angle	Real	Imaginary
I_{1A} (A)	370.0	34.7	304.19	210.63
I_{1B} (A)	370.0	274.7	30.32	−368.76
I_{1C} (A)	370.0	154.7	−334.51	158.12
V_{1A} (kV)	310.8	231.2	−194.75	−242.22
V_{1B} (kV)	310.8	111.2	−112.39	289.77
V_{1C} (kV)	310.8	−8.8	307.14	−47.55

Table VI lists the B-phase fault current and voltage from the event report at Terminal B.

TABLE VI
TERMINAL B VOLTAGE AND CURRENT AT RELAY TRIP INSTANT

	Magnitude	Angle	Real	Imaginary
I_B (A)	146.3	257	−32.91	−142.55
V_B (kV)	310.1	112.7	−119.67	286.08
I_N (A)	266.9	110.2	−92.16	250.48

For the Thèvenin's current calculation, the positive-sequence current of the faulted phase is adjusted to be equal to the measured negative-sequence current, as shown in Table VII.

TABLE VII
POSITIVE SEQUENCES USING THÈVENIN'S CURRENT

	Magnitude (A)	Angle	Comments
I_{2A}	79.50	−9.7	
I_{2B}	79.50	110.3	From Event Report
I_{2C}	79.50	230.3	
I_{1A}	79.50	230.3	
I_{1B}	79.50	110.3	Adopted Equal to I2B
I_{1C}	79.50	−9.7	
I_{0A}	88.97	110.2	
I_{0B}	88.97	110.2	From Event Report
I_{0C}	88.97	110.2	

Again, Thèvenin's current is $I_{Bth} = I_{1B} + I_{2B} + I_{0B}$. The fault current is equal to Thèvenin's current added to the prefault current, as shown in Table VIII.

TABLE VIII
TERMINAL B TOTAL FAULT CURRENT

	Magnitude (A)	Angle
I_F Thev (IB)	247.97	110.26
+		
I Prefault	370.00	−85.30
=		
I_F Total	147.04	−112.20
From Event Report	146.30	−103.00

The calculated current differs by just 0.50 percent from the measured current.

4) Fault Resistance and Fault Location
Using a short-circuit calculation program, protection engineers estimated R_F and the fault location. The system data used for the calculation were obtained from the Brazilian National Interconnected System Operator (ONS). Fig. 4 shows the calculated currents with 528 ohms of R_F.
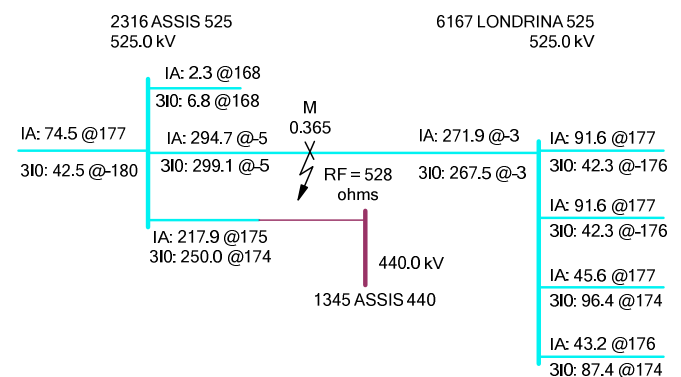
Fig. 4. Fault modeling

Assuming the R_F and fault location as follows, the calculated phase-to-ground currents are quite close to those observed in the real event:

R_F = 528 ohms

Fault location = 0.365 per unit from Terminal A

Table IX compares the real and calculated current values.

TABLE IX
COMPARISON BETWEEN CALCULATED AND MEASURED CURRENTS

	Terminal A		Terminal B	
	Thèvenin (Event Report)	Calculation Program	Thèvenin (Event Report)	Calculation Program
I_B (A)	318.8	294.7	247.97	271.9
I_{Ground} (A)	299.5	299.1	266.90	267.5

The engineers used the zero-sequence network for fault location calculation because it is not influenced by load conditions at the fault instant like the positive-sequence network is. Fig. 5 shows the zero-sequence network, and Table X shows the validation results.
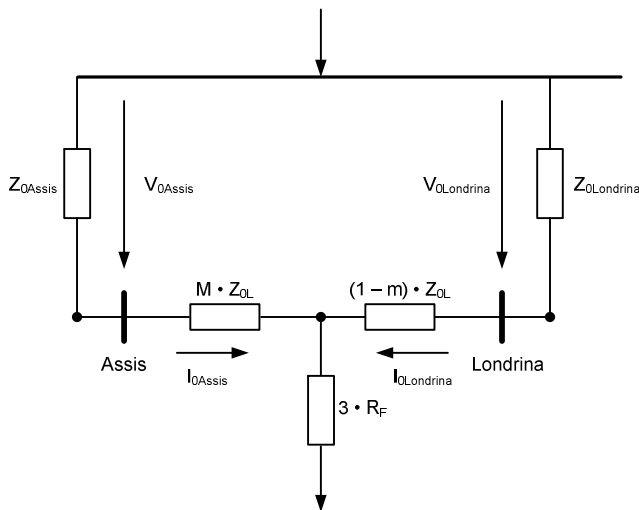
Fig. 5. Zero-sequence network

TABLE X
ZERO-SEQUENCE NETWORK COMPARISON

	Event Report	Calculation Program
V_{0Assis} (V)	6100	6289
I_{0Assis} (A)	299.5	299.1
Z_{0Assis} (Ohms)	61.1	63.0
$V_{0Londrina}$ (V)	2700	2710
$I_{0Londrina}$ (A)	266.9	267.5
$Z_{0Londrina}$ (Ohms)	30.35	30.40

The data used to perform the calculation are accurate. The fault location is estimated as 0.365 per unit from the transmission line. Until this point, the analysts did not know the main cause of the fault; they wanted to confirm that the fault location position was correct.

5) Protective Relay Impedance Calculation

Equation (1) shows the expression to calculate the apparent impedance of the phase-to-ground loop (for B-phase):

$$Z_B = \frac{V_B}{I_B + k_0 \cdot I_N} \tag{1}$$

V_B = B-phase voltage

I_B = B-phase current

I_N = residual (ground) current = 3 $\cdot$ I0

k_0 = zero-sequence current compensation factor

a) Terminal A

As mentioned before, apparent impedance can be calculated according to (1); the engineers used the data from the event report to perform the calculation, and the results are shown in Table XI.

TABLE XI
CALCULATED APPARENT IMPEDANCE

	Magnitude	Angle
V_B (kV)	309.80	110.00
I_B (A)	680.80	112.20
I_N (A)	299.50	100.10
k_0	1.189	−13.89
$k_0 \cdot I_N$	356.11	86.21
$I_B + K_0 \cdot I_N$	1012.98	103.34
Z_B Ohms Primary	305.83	6.66

The calculated apparent impedance has R equal to 303.76 ohms and X equal to 35.48 ohms. This impedance value is beyond the reach of the Zone 3 distance element.

In a case of a fault with no load condition, there is only the Thèvenin's current. The calculated apparent impedance is shown in Table XII.

TABLE XII
CALCULATED APPARENT IMPEDANCE WITH NO LOAD

	Magnitude	Angle
V_B (kV)	309.80	110.00
I_B (A)	318.83	99.69
I_N (A)	299.50	100.10
K_0	1.189	−13.89
$k_0 \cdot I_N$	356.11	86.21
$I_B + K_0 \cdot I_N$	670.29	92.58
Z_B Ohms Primary	462.19	17.42

The calculated apparent impedance has R equal to 305.83 ohms, due to load current influence. With no load, it would be 462.19 ohms.

b) Terminal B

We can calculate the apparent impedance using the data from the event report. The result is shown in Table XIII.

TABLE XIII
CALCULATED APPARENT IMPEDANCE

	Magnitude	Angle
V_B (kV)	310.10	112.70
I_B (A)	146.30	−103.00
I_N (A)	266.90	110.20
K_0	1.189	−13.89
$k_0 \cdot I_N$	317.34	96.31
$I_B + K_0 \cdot I_N$	185.69	111.41
Z_B Ohms Primary	1670.01	1.29

In this situation, the calculated apparent impedance has R equal to 1,669.59 ohms and X equal to 37.54 ohms. This impedance value is beyond the reach of the distance element.

In a case of a fault with no load condition, there is only the Thèvenin's current. The calculated apparent impedance is shown in Table XIV.

TABLE XIV
CALCULATED APPARENT IMPEDANCE WITH NO LOAD

	Magnitude	Angle
V_B (kV)	310.10	112.70
I_B (A)	247.97	110.26
I_N (A)	266.90	110.20
K_0	1.189	−13.89
$k_0 \cdot I_N$	317.34	96.31
$I_B + K_0 \cdot I_N$	561.19	102.43
Z_B Ohms Primary	552.58	10.27

Note again the load influence on the fault.

6) Expression for Phase-to-Ground Impedance

The effect of R_F in a looped line can be seen at [1] and is illustrated in Fig. 6.
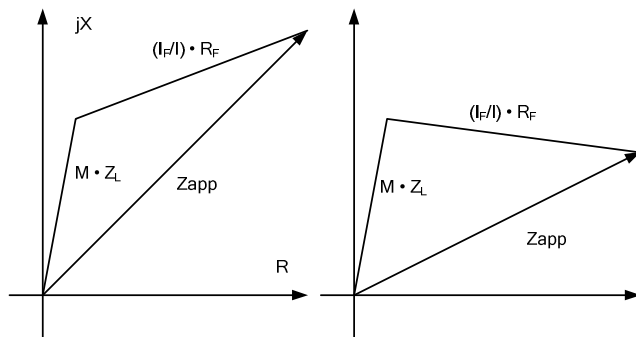
Fig. 6.   Fault impedance effect

Zapp = apparent impedance

Z_L = line impedance

m = fault point (per unit from the protection terminal)

$I_F = I_N + I_{N'}$ = total fault current at the short-circuit point

$I_N = 3 \cdot I0$ current at Terminal A

$I_{N'} = 3 \cdot I0$ current at Terminal B

$I = I_A + k_0 I_N$

I_A = phase current for A-phase fault

The I_F/I ratio can cause an increase in the measured R_F as well as a displacement of the measured resistance angle so that the apparent phase-to-ground impedance can assume high values.

The following expression approximates the phase-to-ground impedance for a nonradial transmission line with an A-phase-to-ground fault with R_F:

$$\frac{V_A}{I_A + k_0 \cdot I_N} = Z_A + \left(\frac{I_N + I_{N'}}{I_A + k_0 \cdot I_N}\right) \cdot R_F \qquad (2)$$

where:

Z_A = Phase A impedance

$m \cdot Z_L$ = line impedance from relay terminal to fault location

I_N = measured ground current at terminal

$I_{N'}$ = measured ground current at remote terminal

I_A = measured phase current at terminal

R_F = fault resistance

Using event reports to estimate the total current $(I_N + I_{N'})$ is difficult because of system nonhomogeneity (different phase references at the two terminals). However, the arithmetic sum is not exactly the fault current across R_F. To get a common phase reference, we would need to use synchrophasors.

For radial transmission lines, there is no $I_{N'}$ and $I_A = In$, so the expression becomes:

$$\frac{V_A}{I_A + k_0 \cdot I_N} = Z_A + \frac{R_F}{1 + k_0} \qquad (3)$$

7) Impedance Analysis

Tables XV and XVI compare the values of event report data, values provided by the short-circuit calculation program, and estimated impedance values from (3) for Terminals A and B.

TABLE XV
IMPEDANCE COMPARISON TERMINAL A IN OHMS

	Z Event Report	Z Calculation Program	Z Estimated by Expression
No Load	462.19	466.27	445
With Load	305.83	–	293

TABLE XVI
IMPEDANCE COMPARISON TERMINAL B IN OHMS

	Z Event Report	Z Calculation Program	Z Estimated by Expression
No Load	552.58	514.70	530
With Load	1670.01	–	1591

The short-circuit calculation program was set for a no-load condition (classic short-circuit calculation). Note that the calculated values are quite close to the ones calculated using voltages and currents measured in the event report with no-load effect.

The calculated R_F from (3) shows values of the same order. For that calculation, it is necessary to have the apparent impedance value at the terminal (taken from the event report), knowledge of the ground currents at the two terminals, and the line impedance from the terminal to the fault point. Therefore, the fault point has to be known or well estimated (4).

$$\text{apparent} = Z_A + \left(\frac{I_N + I_{N'}}{I_A + k_0 \bullet I_N} \right) \bullet R_F \qquad (4)$$

For the fault under analysis, the load current caused the relay at Terminal A to measure a lower impedance, whereas the load current caused the relay at Terminal B to measure a higher impedance. This incorrect impedance measurement remained until one of the breakers opened, causing the fault conditions to change. This incorrect impedance measurement highlights the importance of pilot schemes with ground directional overcurrent elements to detect high-resistance faults.

B. *Analysis of Second Fault*

1) Nature of the Fault
Eleven minutes after the first fault, a new fault was recorded on the same B-phase.

Again, the total fault current had a resistive characteristic. The ground current had the following values:

I_{Ground} (Terminal A) = 457.5 A $\angle$ –6.8° (related to VB)
I_{Ground} (Terminal B) = 410.0 A $\angle$ –3.2° (related to VB)

2) Fault Resistance and Fault Location
Using the same techniques, the following results were obtained:

R_F = 342 ohms
Fault location = 0.365 per unit from Terminal A

Table XVII shows the comparison between the calculated apparent impedance data from the event report and the calculated impedance values provided by the short-circuit calculation program.

TABLE XVII
IMPEDANCE COMPARISON IN OHMS

	Terminal A		Terminal B	
	Z Event Report	Z Calculation Program	Z Event Report	Z Calculation Program
No Load	303.62	303	353.85	335
With Load	227.25	–	631.18	–

Again, the calculated values from the short-circuit program are quite close to the calculated values from the event report, considering a no-load effect and an out-of-reach distance function.

C. *Analysis of Third Fault*

1) Nature of the Fault
About ten minutes after the second fault, there was a third B-phase fault. The ground current had the following values:

I_{Ground} (Terminal A) = 717.2 A $\angle$ –8.1° (related to VB)
I_{Ground} (Terminal B) = 619.2 A $\angle$ –6.2° (related to VB)

2) Fault Resistance and Fault Location
Using the same techniques, the following results were obtained:

R_F = 218 ohms
Fault location = 0.352 per unit from Terminal A

Table XVIII shows the comparison between the calculated apparent impedance data from the event report and the calculated impedance values provided by the short-circuit calculation program.

TABLE XVIII
IMPEDANCE COMPARISON IN OHMS

	Terminal A		Terminal B	
	Z Event Report	Z Calculation Program	Z Event Report	Z Calculation Program
No Load	191.53	191.7	230.91	219.8
With Load	159.28	–	321.08	–

D. *Main Cause of the Faults*

On the day of the faults, the weather conditions were rainy and windy with atmospheric electrical discharges. The possibility of flashover across the insulator to the structure resulting from atmospheric electrical discharge was low, considering the magnitude of the estimated R_F. For flashovers to occur, the R_F must be lower. Even when considering all the ground resistance of structures, the impact to the fault was minimal.

The fault location was calculated to be between 42 and 44 kilometers from Terminal A. At that location, the transmission line crosses over the Paranapanema River. The analysts speculated that the fault could have flashed to the water, assisted by the intense weather conditions.

However, the analysts were still unsure what caused the fault. Because of the high R_F, a tree was ruled out as the cause. Past experience showed typical resistance values of between 30 and 100 ohms primary for faults caused by trees.

E. Analysis of the Protection Performance

The protection performance was correct for all of the faults. The directional ground overcurrent protection on a pilot directional comparison scheme tripped as expected. The directional element's performance and the sensitivity setting for ground faults were satisfactory.

Although the distance elements did not operate, this is considered a correct operation because the fault impedance was outside their zones of operation.

1) Performance of the Negative-Sequence Directional Element

The relay has a negative-sequence element that tests the calculated negative-sequence impedance against forward and reverse thresholds [2].

The transmission line relay settings for the directional control elements at both line terminals are:

Order = Q → negative-sequence polarization

50FP = 0.40 and 50RP = 0.25 → minimum forward and reverse current

Z2F = 1.70 and Z2R = 1.80 → forward and reverse threshold

a2 = 0.10 → minimum I_2/I_1 ratio

Terminal A data for the first short circuit:

PTR = 4565, CTR = 400, PTR/CTR = 4565/400 = 11.41

I_2 = 109.5 A ∠ 99.5° (primary)

I_1 = 476.3 A ∠ 114.5° (primary)

V_2 = 2500 V ∠ –9.7° (primary)

Analysis:

3_{I2} = 3 • 109.5 = 328.5 A (primary) → 0.821 A (secondary)

0.821 > 50FP → okay

I_2/I_1 = 109.2/476.3 = 0.23

0.23 > a2 → okay, negative element active

Line angle Θ = 86.29°

$$Z_2 = \frac{\text{Re}\left[V_2 \bullet (I_2 \bullet 1/\Theta)^*\right]}{|I_2|^2} \qquad (5)$$

Z_2 = –39.02/11.41 = –3.42 ohms (secondary)

Z_2 < Z2F (–3.42 < 1.70) → okay, forward fault

The directional element settings were capable of sensing low currents from very high-resistance faults on the transmission line.

2) Phase Discrimination

The relay had correctly discriminated the faulted B-phase at both ends of the line.

3) Performance of the Fault Location Function

The relay has a fault location function. For very high R_F, there was no set condition for an accurate fault location. The displayed values were not reliable. Synchrophasors improve fault location performance in these cases because they have voltages and currents for both terminals at the same instant of time, with accuracy better than five microseconds.

F. Testing the Negative-Sequence Fault Location System

An interesting fault location method is described in [3] that is not affected by prefault load flow, R_F, power system non-homogeneity, or current infeed from other line terminals.

The algorithm:

$$A \bullet m^2 + B \bullet m + C = 0 \qquad (6)$$

$$A = |I_{2R}|^2 \bullet \left[\text{Re}(Z_{2L})^2 + \text{Im}(Z_{2L})^2\right] - \left[\text{Re}(I_{2S} \bullet Z_{2L})^2 + \text{Im}(I_{2S} \bullet Z_{2L})^2\right] \qquad (7)$$

$$B = -2 \bullet |I_{2R}|^2 \bullet \left[\text{Re}\left(Z_{2R} + Z_{2L}\right) \bullet \text{Re}\left(Z_{2L}\right) + \text{Im}(Z_{2R} + Z_{2L}) \bullet \text{Im}(Z_{2L})\right] - 2 \bullet \left[\text{Re}(I_{2S} \bullet Z_{2S}) \bullet \text{Re}(I_{2S} \bullet Z_{2L}) + \text{Im}(I_{2S} \bullet Z_{2S}) \bullet \text{Im}(I_{2S} \bullet Z_{2L})\right] \qquad (8)$$

$$C = |I_{2R}|^2 \bullet \left[\text{Re}(Z_{2R} + Z_{2L})^2 + \text{Im}(Z_{2R} + Z_{2L})^2\right] - \text{Re}(I_{2S} \bullet Z_{2S})^2 - \text{Im}(I_{2S} \bullet Z_{2S})^2 \qquad (9)$$

m = distance (per unit of transmission line)

V_{2S} = sending end negative-sequence voltage

V_{2R} = receiving end negative-sequence voltage

I_{2S} = sending end negative-sequence current

I_{2R} = receiving end negative-sequence current

Z_{2L} = negative-sequence transmission line impedance

Z_{2R} = receiving end negative-sequence source impedance = $-V_{2R}/I_{2R}$

Z_{2S} = sending end negative-sequence source impedance = $-V_{2S}/I_{2S}$

For the first short circuit:

Z_{2L} = 2.50 + j 38.65 ohms primary

V_{2S} = 3600 V ∠ –9.7° (primary)

I_{2S} = 109.5 A ∠ 99.5° (primary)

V_{2R} = 3200 V ∠ 30.8° (primary)

I_{2R} = 79.5 A ∠ 110.3° (primary)

Results:

A = –8505411.08

B = –67490470.78

C = 25864855.38

m_1 = 0.366 from Terminal A

m_2 = –8.30132944

The terms m_1 and m_2 are the two possible solutions for m from (6); the negative value is disregarded.

Note that the negative-sequence fault location algorithm, using data from the two terminals, is quite accurate for very high-resistance faults.

III. NEW FAULTS IN AUGUST 2006

On August 16, 2006, two faults were recorded (at 2:00 p.m. and 2:04 p.m.), with the transmission line opening and reclosing in both cases. At the time, a line maintenance team observed the flashover from the transmission line and the vegetation close to the Paranapanema River, as shown in Fig. 7.

Fig. 7.   Fire damage visible at fault location

The first fault was a B-phase-to-ground fault with high impedance (R_F = 350 ohms), and the operation of the ground overcurrent directional comparison scheme was correct. Four minutes after the first occurrence, a second fault occurred at the same phase (R_F = 34 ohms), and the distance protection element tripped the transmission line.

A. Analysis of First Fault

1) Nature of the Fault

This fault involved a tree and was characterized by very high resistance. The faulted phase voltage and current and the residual current are displayed in Fig. 8.
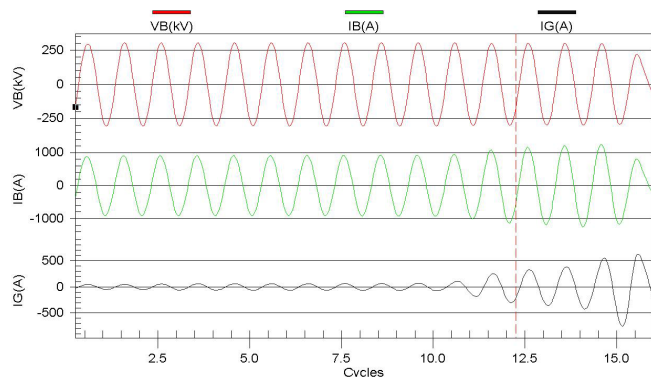
Fig. 8.   VB, IB, and IG waveforms

The voltage was essentially maintained during the fault with the following ground currents:

I_{Ground} (Terminal A) = 446.9 A ∠ –10.4° (related to VB)

I_{Ground} (Terminal B) = 400.9 A ∠ –6.3° (related to VB)

2) Fault Resistance and Fault Location

Using the same techniques, the following results were obtained:

R_F = 350 ohms

Fault location = 0.365 per unit from Terminal A

Table XIX shows the comparison between the values of calculated apparent impedance using data from the event report and the calculated impedance value provided by the short-circuit calculation program.

TABLE XIX
IMPEDANCE COMPARISON IN OHMS

	Terminal A		Terminal B	
	Z Event Report	Z Calculation Program	Z Event Report	Z Calculation Program
No Load	303.02	310	363.42	343
With Load	170.8	–	1125.39	–

B. Analysis of Second Fault

1) Nature of the Fault

It was observed, in this case, that the B-phase-to-ground fault involving a tree was a classic short circuit with high current and voltage sag at faulted phase, as shown in Fig. 9.
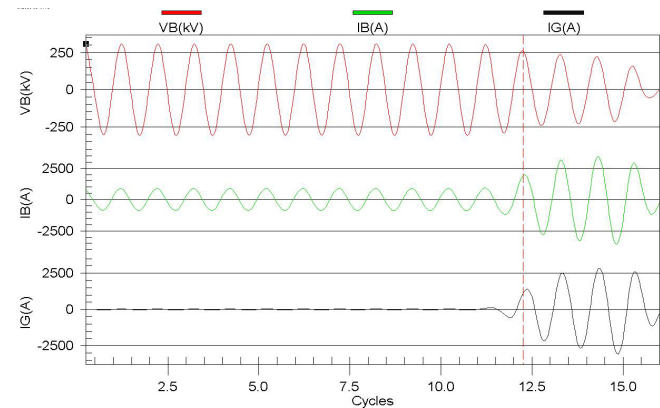
Fig. 9.   VB, IB, and IG waveforms show more current and voltage sag at the fault due to the lower impedance fault

The ground currents measured in the event report are:

I_{Ground} (Terminal A) = 2.914 A ∠ –23.3° (related to VB)

I_{Ground} (Terminal B) = 2.569 A ∠ –26.7° (related to VB)

2) Fault Resistance and Fault Location

Using the same techniques as before, the following results were obtained:

R_F = 34 ohms

Location = 0.359 per unit of Terminal A

3) Impedance Calculation

From the event report, we can calculate the apparent impedance, as shown in Table XX.

TABLE XX
RELAY APPARENT IMPEDANCE IN OHMS

Z_B Ohms Primary	Magnitude	Angle
Apparent	32.87	24.60
No Load	35.07	31.25

Fig. 10 shows the calculated impedances, from Table XX, in comparison to the reach of the distance zones. Out of all of the occurrences described in this paper, this event is the only one for which the distance protection function tripped the transmission line.

The fault locator of the relay indicated 47 kilometers for a 44.8-kilometer location.
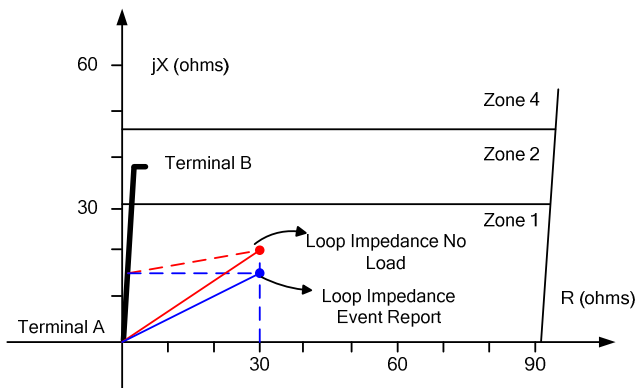
Fig. 10. Distance element and fault point at Terminal A

For Terminal B, the apparent impedances are listed in Table XXI.

TABLE XXI
RELAY APPARENT IMPEDANCE IN OHMS

Z_B Ohms Primary	Magnitude	Angle
Apparent	51.91	40.89
No Load	47.32	33.54

The calculated reactance shows the influence of the load. With load, the apparent impedance is inside Zone 2. Without load, the fault would be in Zone 1 (physically to 64 percent of the transmission line). The fault locator indicated 76.9 kilometers for a 78-kilometer location, as shown in Fig. 11.
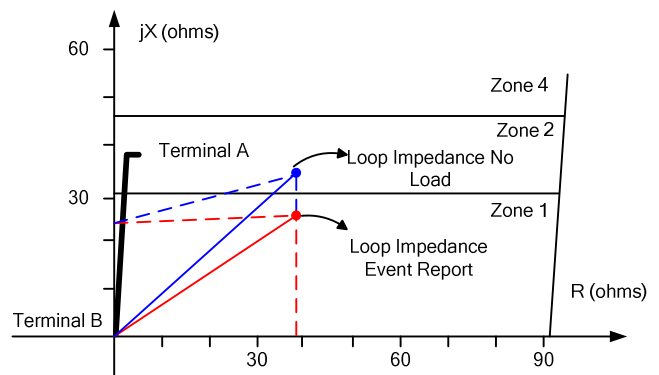
Fig. 11. Distance element and fault point at Terminal B

C. Considerations on the Primary Cause of the Faults

Fig. 7 and the fault locations shown before prove that there was a phase-to-ground fault involving a tree, and the analysts concluded that the July 2006 faults were caused by the same tree. Fault resistances between 528 ohms (first fault of July) and 34 ohms (last fault in August) were observed.

These data prove that there can be a fault-to-ground with very high resistance, even if the fault is through vegetation.

IV. DIRECTIONAL GROUND OVERCURRENT FUNCTION ON PILOT DIRECTIONAL COMPARISON SCHEME

As demonstrated in this paper, the ground directional overcurrent protection function of a directional comparison scheme identified and tripped the feeder on four occasions. It was the only function that detected the high-impedance faults. The two transmission line protection functions in the duplicated scheme meet the established application criteria specified by Brazilian electrical sector authorities. The directional ground overcurrent function used in a pilot scheme has the following advantages:

- It is sensitive enough to detect low-magnitude ground faults due to low currents resulting from high-impedance faults.
- It provides fast tripping of the protected line, considering the time requirements.
- It provides reliable overall protection, depending on the reliability of the communications media between the line terminals.

We cannot expect distance functions to detect all possible transmission line faults, so those functions need complementary ground fault protection.

It is certainly possible to have ground faults with very low currents and extremely high resistance—not suitable for detection even by ground overcurrent relays. Recent studies about these types of protection are mentioned in [1].

V. DIFFERENTIAL FUNCTION AS MAIN PROTECTION FOR A TRANSMISSION LINE

An alternative for line protection is the use of the differential function as the main protection and the distance and/or directional overcurrent functions as backup protection. Differential protection presents the following advantages:

- It is as sensitive to high-impedance fault detection as the ground overcurrent function is, due to new negative-sequence and three-phase-sequence characteristics.
- It is selective.
- The discrimination of the faulted phase is inherent for segregated protection or eventually for protection with a phase discrimination algorithm.
- It does not require voltage information.
- It presents high sensitivity for phase faults.
- It is immune to:
  - Blown potential fuse conditions.
  - Power oscillations through the protected line.
  - Mutual coupling effects.
  - Series unbalance.

One of the few disadvantages of differential protection for a transmission line is the demand for a highly reliable and fast communications link (fiber optic—dielectric or optical ground wire) between the line terminals. This is an economical disadvantage for long lines.

There is a tendency to use differential protection only for short lines (up to 20 kilometers). However, it should be observed that the evolution of technology and the introduction of digital microprocessor-based relays have brought about more resources, different philosophies, and reliable fault detection and decision schemes. Through fiber-optic communication, differential protection can be applied in lines of any length. So, the paradigm associating differential protection only with short lines is no longer true.

VI. CRITERIA FOR RESISTIVE REACH SETTING OF A QUADRILATERAL GROUND DISTANCE FUNCTION

A. Suggestion

In the past, Brazilian protection practices tended to use settings for the lateral reach of a quadrilateral characteristic for ground faults with values less than 60 ohms primary. This practice was the result of not having enough information to calculate or even correctly evaluate the value of R_F. During the 1970s and 1980s, values around 20 to 60 ohms primary for R_F were commonly used.

The tendency to consider the occurrence of high-impedance ground faults more probable for medium-voltage systems reinforced this practice. For EHV systems, the probability was considered smaller or even impossible.

With the advent of digital technology, more flexible calculation tools, and the extensive use of event reports, analysts began to observe that ground faults could have larger R_F at any level of voltage.

B. Caution

Protective relay literature, mainly from manufacturers, often shows the criteria to determine the setting limit for resistive reach with line impedance $(R + jX)$ and the Zone 1 setting.

For instance, the appendix in [4] shows that the reactive reach can have an overreach effect depending on its settings, mainly due to the angle error from potential transformers but also due to the system nonhomogeneity, load conditions, and inherent relay errors. For example, a fault at the remote busbar can have the same reactance measured inside the first reactance zone. The error can be compensated through a bias for the polarization angle or through the reduction of the reactive reach for Zone 1 [4].

The resistive reach setting does not affect the reactive reach. In the case of a fault with R_F at the resistive reach setting limit, a reactive reach measurement error of the mentioned angle error can happen [4].

Finally, note that the maximum limit recommended for the resistive reach for ground faults is very important in selecting the pilot protection philosophy used for the distance function. A permissive scheme usually allows higher settings for resistive reach because the Zone 1 tripping will depend on the permission of the remote terminal protection.

VII. CONCLUSION

A. Events

During all of the events discussed in this paper, the line protection performed correctly, detecting the very high-impedance faults through the directional ground overcurrent functions operating on a directional comparison pilot scheme. The distance functions did not trip (except for the last fault analyzed), and they would not have conditions to trip when fault resistances were very high.

The directional element, based on a principle that calculates negative-sequence impedance and tests the result against thresholds, presented a good directional sensitivity for all the analyzed faults.

The phase discrimination algorithm performed perfectly for the very high-resistance phase-to-ground faults.

The single terminal-based fault location design for regular line protection relays does not perform satisfactorily during very high-resistance faults.

This paper demonstrated that the two- or three-terminal negative-sequence fault location algorithm presented in [3] is quite precise for very high-resistance faults.

B. Analysis Techniques

The influence of the prefault load condition is significant for the impedance measurement made by the distance function. An event report can have enough data for calculating the measured impedance by the distance function at actual load condition, while a classical fault short-circuit program can calculate the fault conditions without the load influence.

Using this calculation software, the resistance of a ground fault can be estimated, or it can be calculated through an

expression, since both the extremities fault values and the approximate distance to the fault point are available.

Techniques of fault analysis allow analysts to separate the pure fault current (Thèvenin) and the prefault load current. It is possible to determine the theoretical values of impedance that a distance function would measure if there was no load. It is also possible to compare the calculated conditions by a short-circuit program with what actually happens in a disturbance.

Synchrophasors can improve and speed the event analysis and make it more accurate.

C. Fault Resistance

Fault resistances to ground on the order of hundreds of ohms primary are possible, even in an EHV transmission line. This situation exists more commonly than believed because of the direct association to ground faults through vegetation.

A characteristic of such faults is the occurrence of repetitive ground faults, presenting smaller R_F for each subsequent fault in a shorter interval of time.

D. Resistive Reach Setting Criteria

For the resistive setting of the quadrilateral characteristic of a ground distance function, research has recommended to adopt, on average, a value of at least 80 ohms primary for HV and EHV transmission lines of any voltage level for lines with pilot protection.

Existing recommendations from protective relay manufacturers should be observed to avoid Zone 1 overreaching.

E. Transmission Line Protection

A distance function is never self-sufficient in transmission line protection; proper protection always demands a complementary ground directional overcurrent function and pilot scheme.

Due to distance function limitations, it is always recommended to evaluate the use of a differential function for a nonradial transmission line with distance functions as backup, even for long lines, for any voltage level at which a reliable communications channel is available.

VIII. REFERENCES

[1] R. Abboud, W. F. Soares, and F. Goldman, "Challenges and Solutions in the Protection of a Long Line in the Furnas System," proceedings of the 32nd Annual Western Protective Relay Conference, Spokane, WA, October 2005. Available: http://www.selinc.com/techpprs.htm.

[2] J. Roberts and A. Guzmán, "Directional Element Design and Evaluation." Available: http://www.selinc.com/techpprs.htm.

[3] D. A. Tziouvaras, J. Roberts, and G. Benmouyal, "New Multi-Ended Fault Location Design for Two- or Three-Terminal Lines." Available: http://www.selinc.com/techpprs.htm.

[4] E. O. Schweitzer, III, K. Behrendt, and T. Lee, "Digital Communications for Power System Protection: Security, Availability, and Speed," pp. 22–24. Available: http://www.selinc.com/techpprs.htm.

IX. FURTHER READING

"High Impedance Faults," CIGRE Study Committee B5, Report Nr. SC B5/WG94 DFR-r2.0, 2008.

SEL-421 Reference Manual. Available: http://www.selinc.com/instruction_manual.htm.

E. O. Schweitzer, III and J. Roberts, "Distance Relay Element Design," proceedings of the 46th Annual Conference for Protective Relay Engineers, College Station, TX, April 1993.

J. Mooney and J. Peer, "Application Guidelines for Ground Fault Protection," proceedings of the 24th Annual Western Protective Relay Conference, Spokane, WA, October 1997.

X. BIOGRAPHIES

Paulo K. Maezono received his BSEE from the University of São Paulo Polytechnic School of Engineering, Brazil, in 1969. He attended the "Power Technology Course" at Power Technologies Inc. in Schenectady, New York, in 1974. He earned an MSEE degree from the Federal School of Engineering of Itajuba in 1978. From 1972 to 1985, he served as assistant professor at the Mackenzie University School of Engineering in São Paulo. His professional experience from 1970 to 1997 includes electrical engineering work and management at CESP, a utility company of the State of São Paulo. Since 2000, he has been with Virtus as founder and senior consultant in protective relaying and disturbance analysis, with a group of associated consultants. He is a member of IEEE and Cigré.

Enrique Altman received his BSEE degree from the University of Misiones, Argentina, in 2004. Since 2005, his professional experience includes working as an electrical engineer and manager at TRANSENER, which is an operation and maintenance company of electrical power systems.

Kennio Brito Guimarães received his BSEE from Universidade do Estado de Minas Gerais in 2003. He served at CEMAT and Jalapão/Celg in 2004 in the distribution area. In 2005, he joined Transener Internacional Ltda. as a maintenance engineer. His responsibilities include all the extra-high-voltage equipment in the transmission department

Vanessa Alves dos Santos Mello Maria received her BSEE from Federal University of Rio de Janeiro, Brazil, in 2004. She earned an MSEE degree from COPPE/Federal University of Rio de Janeiro in 2007. She joined ATE Transmissora de Energia S.A. in 2005 as an electrical engineer in the power system operation department. Her responsibilities include analysis of power systems in the ATE grid.

Fabiano Magrin received his BSEE from Universidade Estadual de Campinas, UNICAMP, in 2003. He joined Schweitzer Engineering Laboratories, Inc. (SEL) upon graduation as a field application engineer. His responsibilities include training and assisting SEL customers in protection and automation efforts related to transmission, distribution, generation, and industrial applications. He is a member of the Cigré Study Committee B5 in Brazil.